analytical chemistry

Letter

pubs.acs.org/ac

High-Sensitivity Rheo-NMR Spectroscopy for Protein Studies

Daichi Morimoto,[†] Erik Walinda,[‡] Naoto Iwakawa,[†] Mayu Nishizawa,[†] Yasushi Kawata,[#] Akihiko Yamamoto,[§] Masahiro Shirakawa,[†] Ulrich Scheler,[∥] and Kenji Sugase*[,†]

[†]Department of Molecular Engineering, Graduate School of Engineering, Kyoto University, Kyoto-Daigaku Katsura, Nishikyo-ku, Kyoto 615-8510, Japan

[‡]Department of Molecular and Cellular Physiology, Graduate School of Medicine, Kyoto University, Yoshida Konoe-cho, Sakyo-ku, Kyoto 606-8501, Japan

[#]Department of Chemistry and Biotechnology, Graduate School of Engineering, Tottori University, 4-101 Koyama-cho Minami, Tottori 680-8552, Japan

[§]Bruker BioSpin K.K., 3-9 Moriya-cho, Kanagawa-ku, Yokohama, Kanagawa 221-0022, Japan

[∥]Leibniz-Institut für Polymerforschung Dresden e.V., Hohe Strasse 6, D-01069 Dresden, Germany

Supporting Information

ABSTRACT: Shear stress can induce structural deformation of proteins, which might result in aggregate formation. Rheo-NMR spectroscopy has the potential to monitor structural changes in proteins under shear stress at the atomic level; however, existing Rheo-NMR methodologies have insufficient sensitivity to probe protein structure and dynamics. Here we present a simple and versatile approach to Rheo-NMR, which maximizes sensitivity by using a spectrometer equipped with a cryogenic probe. As a result, the sensitivity of the instrument ranks highest among the Rheo-NMR spectrometers reported so far. We demonstrate that the newly developed Rheo-NMR instrument can acquire high-quality relaxation data for a protein under shear stress and can trace structural changes in a protein during fibril formation in real time. The described approach will facilitate rheological studies on protein structural deformation, thereby aiding a physical understanding of shear-induced amyloid fibril formation.

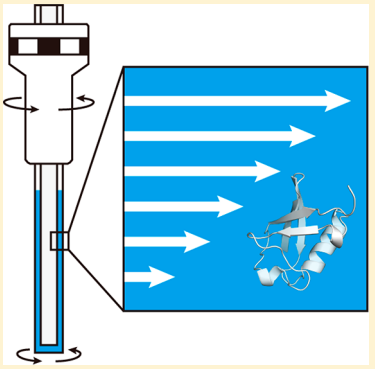

Structural deformation of proteins occurs in response to physical or chemical stress. Not only isotropic stress, such as changes in temperature and pressure, but also anisotropic physical stress can cause structural deformation of proteins and result in protein aggregation. Indeed, several amyloid-prone proteins such as β-lactoglobulin and insulin are known to form pathological protein fibrils in response to unidirectional physical stress.[1−3] In addition, directional stress is likely to influence rotational-translational motion and, in turn, the intermolecular associations and interactions of a protein; however, the behavior of proteins under directional physical stress remains relatively unexplored.

Rheo-NMR spectroscopy is the method of choice to investigate the behavior of macromolecules under unidirectional stress at atomic resolution. It was initially established by Nakatani and co-workers to study the rheological properties of polymers.[4] Schmidt and co-workers demonstrated the application of Rheo-NMR to the study of phase transitions in complex fluidic and lamellar systems.[5−8] In addition, the effect of shear stress on polymer dynamics has also been studied by NMR relaxation experiments.[9] Accordingly, most of the current Rheo-NMR studies have investigated polymer samples, in which the repeating units have low molecular weight and are present at high concentration; thus, one does not require a high magnetic field to separate individual NMR resonance lines. In contrast, severe signal broadening and overlap are problematic in NMR experiments for biological macromolecules. To date, only a few biological applications of Rheo-NMR have been reported;[10,11] however, owing to its low sensitivity, state-of-the-art Rheo-NMR spectroscopy cannot provide detailed structural and dynamical information on dilute and/or moderately large molecular weight protein samples. In this study, we have established a novel Rheo-NMR approach that possesses the sufficient sensitivity to observe protein dynamics under sheared conditions and trace atomic-level structural changes during protein fibril formation.

EXPERIMENTAL SECTION

Protein Preparation. Human ubiquitin and M1-linked hexa-ubiquitin were expressed in *Escherichia coli* strain BL21 (*DE3*), which was grown in M9 minimal medium containing 99% ^{15}N-labeled ammonium chloride (Cambridge Isotope Laboratories); in the case of hexa-ubiquitin, the M9 medium also contained 99% U−^{13}C-labeled D-glucose (Cambridge Isotope Laboratories). Ubiquitin was purified by cation exchange and size-exclusion chromatography. M1-linked hexa-

Received: May 15, 2017
Accepted: June 30, 2017
Published: June 30, 2017

DOI: 10.1021/acs.analchem.7b01816
Anal. Chem. 2017, 89, 7286−7290

ubiquitin was expressed as a fusion protein with a C-terminal hexa-histidine (His_6) tag. After cleavage of the His_6 tag by ubiquitin carboxyl-terminal hydrolase YUH1, hexa-ubiquitin was further purified by size-exclusion chromatography. Protein purity was checked by SDS-PAGE.

Rheo-NMR Spectroscopy. All experiments were performed at 298 K on an Avance 600 MHz NMR spectrometer equipped with a 5 mm $^{15}N/^{13}C/^{1}H$ z-gradient triple resonance cryoprobe (Bruker BioSpin). For a stationary inner rod, a magic-angle-spinning (MAS) transfer tube for an Avance 600 MHz NMR spectrometer (Bruker BioSpin), a 12 mm-to-3 mm polytetrafluoroethylene (PTFE) straight union reducer connector (FLON INDUSTRY), and a 173 mm length Pyrex glass stick with a 3 mm outer diameter (Shigemi) were used. Since the inner rod provides an additional surface, its chemical properties may affect protein aggregation propensity. To prepare an outer tube, a 155 mm length NMR tube with a 4.1 mm inner diameter (Shigemi) and a 5 mm Type A ceramics spinner for standard bore shim systems (Bruker BioSpin) were used. The lengths of an NMR tube and a glass stick were determined in pilot experiments. To establish a Rheo-NMR Couette cell in an NMR tube, the length of a glass stick was adjusted to a distance of approximately 1 mm from the inner bottom of an NMR tube. In addition, the length of an NMR tube should be shorter than 155 mm to avoid the collision between the NMR tube and the reducer connector connected to a MAS transfer tube. In all NMR experiments, the sample volume was 0.3 mL. This volume is adequate for automatic gradient shimming. A technical description of the Rheo-NMR instrument is shown in Figure S1. Because a glass stick is inserted in the NMR tube, the sample volume to be detected in the probe coil decreases by 54% (Figure 1, right lower).

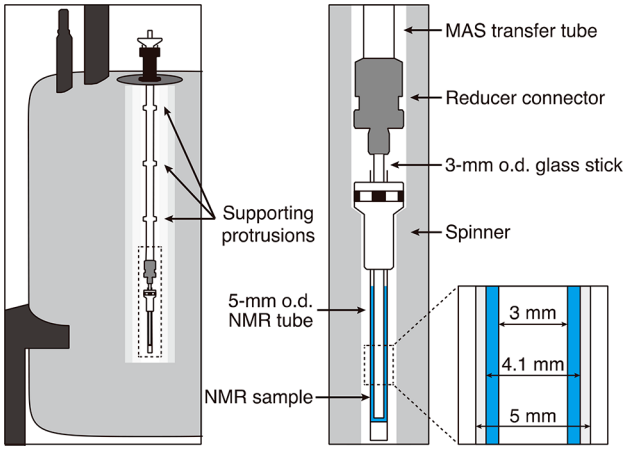

Figure 1. Simple and inexpensive approach to Rheo-NMR spectroscopy. Schematic depiction of the Rheo-NMR instrument (left) with an enlarged view of the geometry of the NMR sample tube (right).

Experiments indicated a 40% decrease in the signal-to-noise ratio compared to a standard solution NMR setup without the inner glass stick (Supplementary Methods). To exclude any effect of impurities of the glass stick on the protein samples, the glass stick was rigorously cleaned before every experiment.

Fluorescence Spectroscopy. Thioflavin T fluorescence was quantified on a FluoroMax4 (HORIBA) spectrometer at 298 K by excitation at 440 nm with acquisition of emission spectra over wavelengths from 460 to 550 nm with a slit width of 5 nm. Samples were diluted to a final concentration of 5 μg/mL in 20 mM potassium phosphate, 5 mM KCl, 1 mM EDTA, 150 mM NaCl, 10% D_2O at pH 6.8, and 25 μM Thioflavin T. The spectral contribution of the buffer was subtracted from the acquired spectra.

Transmission Electron Microscopy. TEM images were obtained by using a JEM-1400Plus instrument (JEOL). The sample was loaded onto a collodion-coated grid and negatively stained with EM Stainer (Nisshin EM).

Graphical Presentation of Rheo-NMR data. The total peak volume in the aliphatic region of the $^{1}H-^{13}C$ HSQC spectra (^{1}H, from 3.28 to −0.35 ppm; ^{13}C, from 42.20 to 5.50 ppm) was 1337409589 and 562939110 in the static and 16 h sheared conditions, respectively. To distinguish chemical shift differences, the lowest contour level of the spectrum in the 16 h sheared condition was set to be 0.42 times lower than that in the static condition, so that the average peak volume was the same in the superimposed spectra. The number of contour levels was set to the same value in a single figure showing spectra taken under the static and sheared conditions.

RESULTS AND DISCUSSION

Novel Rheo-NMR Methodology. To resolve the sensitivity issue of existing Rheo-NMR spectrometers, we have developed a novel Rheo-NMR methodology that can be adapted to any NMR spectrometer, even those equipped with a cryogenic probe (cryoprobe). Previously reported approaches to Rheo-NMR require attachment and detachment of the probe when exchanging a sample tube;[10,12] however, this is impractical for a cryoprobe due to cost and time constraints. Rheo-NMR hardware that does not require attachment and detachment has been reported;[11,13] however, that hardware has not yet been applied to an NMR instrument equipped with a cryoprobe. We therefore developed a simpler and more versatile accessory for Rheo-NMR (Figure 1). We focused on the sample spinning control system, which is a default feature of commercial NMR instruments. An outer-rotating Couette cell can be established by inserting a stationary rod into an NMR tube (outer cylinder) and rotating only the NMR tube using the spinning system. For the stationary rod, we used a MAS transfer tube, which is normally used for inserting and ejecting a solid-state NMR sample tube. The MAS transfer tube fits perfectly inside the upper shim stack in the vertical bore (Figure 1). A 3 mm outer diameter (o.d.) glass stick is connected to the bottom of the MAS transfer tube via a reducer connector, which fixes the position of the glass stick in the center of the MAS transfer tube (Figure 1). After the 5 mm o.d. NMR tube (inner diameter, 4.1 mm) containing the sample solution is placed in the NMR magnet in the normal manner, the glass stick (o.d., 3 mm) connected to the MAS transfer tube is carefully inserted. As a result, the outer-rotating Couette cell is established. A technical description of our Rheo-NMR instrument is presented in Figure S1.

As compared with previous methodologies, this approach significantly simplifies the equipment setup and reduces the cost of constructing a Rheo-NMR system. In addition, we found that, owing to its weight, a ceramic spinner causes much less vibration than a standard spinner. Therefore, automatic gradient shimming along the z-axis can be performed, as in the case of a regular NMR sample tube, and the lock signal (deuterium signal of the solvent) remains stable during the spinning, indicating that the influence of vibration on the measurements is minimized. To the best of our knowledge, this

DOI: 10.1021/acs.analchem.7b01816
Anal. Chem. 2017, 89, 7286−7290

approach is the simplest, most convenient, and most inexpensive Rheo-NMR methodology reported to date.

Validation of Sensitivity and Stability. The high sensitivity of the cryoprobe-based Rheo-NMR instrument enables protein NMR measurements that were previously not attainable by existing Rheo-NMR systems. Indeed, the signal-to-noise ratio of the 600 MHz NMR spectrometer equipped with the cryoprobe was found to increase by 4.2-fold compared to that equipped with the room-temperature probe. To evaluate the sensitivity and stability of the instrument, we investigated the effect of shear stress on the structural dynamics of ubiquitin by measuring ^{15}N R_1, R_2 relaxation rates and $^{1}H-^{15}N$ heteronuclear NOE values for each amino acid residue of ubiquitin. At a spinning frequency of 35 Hz (shear rate, 510–950 s^{-1}; Supporting Information), the relaxation data acquired under sheared and static conditions were of equally high quality, showing that the process of spinning itself barely decreases the quality of data (Figure 2). We found that the

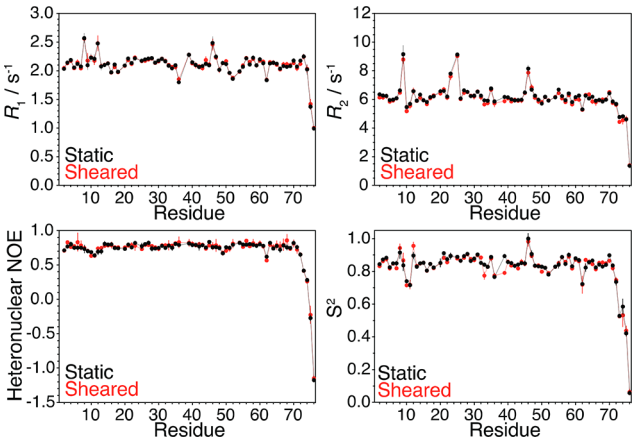

Figure 2. Relaxation data obtained by high-sensitivity Rheo-NMR. Comparative analysis of ^{15}N R_1, R_2 relaxation rates, $^{1}H-^{15}N$ heteronuclear NOE values, and the order parameter S^2 of ubiquitin under static (black) and sheared conditions (red).

applied shear stress caused very small chemical shift changes of cross-peaks in the $^{1}H-^{15}N$ HSQC spectrum (Figure S2). Similarly, we observed no significant overall difference in the relaxation rates or heteronuclear NOE values of ubiquitin between the static and sheared conditions (Figure 2), which may indicate that there was no significant change in the sample temperature due to the shear. Furthermore, analysis of the relaxation data using the program ROTDIF[14] allowed us to obtain the order parameter for each residue (Figure 2) and the overall rotational diffusion parameters (Table S1) under static and sheared conditions. Because there were certain subtle differences in the obtained rotational diffusion parameters (Table S1), it is possible that the applied shear flow disturbed the intrinsic rotational diffusion behavior of the protein. However, a physical theory to support this hypothesis has not been established yet. Taken together, the high sensitivity and stability of the established cryoprobe-based Rheo-NMR instrument have been validated by relaxation experiments on ubiquitin. The acquisition of high-quality data on protein samples will contribute to understanding of the molecular behavior of a protein under the effect of directional stress.

Atomic-Level Analysis of Amyloid Formation. Next, we applied the newly established Rheo-NMR instrument to study a pathologically relevant process, amyloid fibril formation. To date, the structural and kinetical properties of fibril formation have been well characterized; however, no existing method can capture aggregate nucleation and subsequent growth at atomic resolution. It is therefore necessary to establish a method that can observe amyloid fibril formation *in situ* at the atomic level. The cryoprobe-based Rheo-NMR may be one promising approach for monitoring fibril formation at atomic resolution; therefore, we tested if amyloid fibrils can be formed and structural changes during fibril formation can be traced using our instrument. To this end, we used M1-linked hexa-ubiquitin (51 kDa), which forms amyloid-like fibrils upon the application of shear stress.[15] First, we observed that application of shear stress inside the Rheo-NMR Couette cell resulted in the formation of amyloid fibrils of hexa-ubiquitin (Figure 3). This is

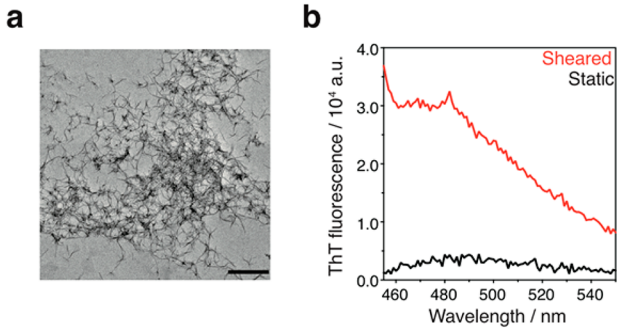

Figure 3. Amyloid-like fibrils of sheared hexa-ubiquitin as formed in the Rheo-NMR experiments. (a) Electron microscopy image of sheared M1-linked hexa-ubiquitin. Bar, 200 nm. (b) Thioflavin-T fluorescence emission spectra of static (black) and sheared (red) M1-linked hexa-ubiquitin.

similar to the previous finding that silk fibroin forms β-sheet-rich structures under moderate shear.[10] In addition, real-time NMR analysis indicated that shear stress at a spinning frequency of 35 Hz led to a decrease in the volume of all cross-peaks in the $^{1}H-^{13}C$ and $^{1}H-^{15}N$ HSQC spectra (Figure S3), confirming the conversion of NMR-observable monomers into amyloid-like fibrils *in situ*. By contrast, no change in cross-peak volume was observed in experiments without applied shear stress (Figure S3). In general, formation of amyloid-like fibrils is irreversible and the fibrils are physicochemically stable once formed. Accordingly, after the spinning was terminated, no further decrease in peak volume occurred (Figure S3), which supported that the decrease in peak volume was due to the applied shear in the Rheo-NMR instrument. In the case of hexa-ubiquitin, structural deformation appears to be a critical step in the fibril formation, but it is unknown which ubiquitin subunit of hexa-ubiquitin is deformed first and how many subunits need to be modified to trigger fibril formation. Therefore, the duration of lag phase is likely modulated by the stochastic nature of nucleation, resulting in different lag times (Figure S3). A key difference to other methods such as Thioflavin T or Congo red assays is that NMR detects various changes in chemical environment throughout the fibril formation process; therefore, any kind of oligomerization or chemical exchange in the lag phase of fibrillation leads to an observable signal loss. In the formation of amyloid fibrils, a series of molecular events, including primary nucleation, fibril elongation, and fragmentation, are thought to take place.[16] In particular, in the cases of natively folded proteins, global or partial deformation of their tertiary structures occurs prior to

DOI: 10.1021/acs.analchem.7b01816
Anal. Chem. 2017, 89, 7286–7290

primary nucleation.[17] Accordingly, our observations suggest that high-sensitivity Rheo-NMR can quantify the amount of the native state of a protein and monitor its changes during fibril formation, which will aid elucidation of the kinetics of multistep fibrillation reactions.

We further examined whether high-sensitivity Rheo-NMR can provide detailed structural information during the fibril formation process. In real-time $^{1}H-^{15}N$ HSQC spectra, essentially no changes in the chemical shift of cross-peaks were detected (Figure S4). In stark contrast, we observed changes in the chemical shift of cross-peaks in real-time $^{1}H-^{13}C$ HSQC spectra (Figure 4). Intriguingly, the affected

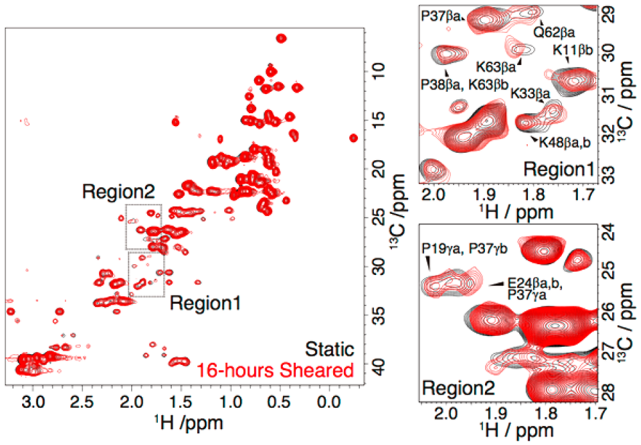

Figure 4. Cross-peak changes in the aliphatic region of hexa-ubiquitin caused by shear-induced fibril formation. $^{1}H-^{13}C$ HSQC spectra of static (black) and sheared (red) hexa-ubiquitin at a spinning frequency of 35 Hz for 16 h. To distinguish chemical shift differences, the lowest contour level of the spectrum in the 16 h sheared condition was set to be 0.42 times lower than that in the static condition. Enlarged views of boxed regions 1 and 2 are shown in the right. Resonance assignments were derived from entry 17769 in the Biological Magnetic Resonance Bank.

cross-peaks correspond to surface-exposed residues of ubiquitin subunits in hexa-ubiquitin that contain all three proline residues of ubiquitin (Figure S5). A previous study indicates that cis–trans isomerization of proline residues is coupled with conformational changes to generate precursors of amyloid fibrils,[18] suggesting that the isomerization may play an essential role in the nucleation of polyubiquitin fibrils; a detailed analysis of structural changes in the fibril formation will be reported elsewhere. Collectively, the high sensitivity of the cryoprobe-based Rheo-NMR instrument enabled us to detect detailed structural changes of protein samples under applied shear stress. Indeed, we obtained site-specific structural information on sheared hexa-ubiquitin, thereby gaining insight into mechanism underlying amyloid fibril formation at atomic resolution.

CONCLUSIONS

Unlike most standard approaches in which drastic physico-chemical conditions such as high temperature, acidic pH, or denaturing agents at high concentration are applied to a sample, our Rheo-NMR instrument observes proteins under nearly physiological conditions: namely, neutral pH, atmospheric pressure, and room temperature (298 K). In addition, the sensitivity of the cryoprobe-based Rheo-NMR ranks highest among the Rheo-NMR spectrometers reported so far, enabling us to acquire high-quality structural information that has been difficult to obtain by previous methodologies. Therefore, it is possible to monitor protein aggregation and fibril formation at atomic resolution, unlike other methods such as fluorescence and circular dichroism spectroscopy. Furthermore, it has been reported that shear forces induce conformational changes in proteins such as von Willebrand factor[19] and (GP)Ib-IX complex;[20] therefore, this approach to Rheo-NMR provides a way to conduct any kind of NMR experiments of proteins under the effects of unidirectional physical stress.

In mammalian cells, proteins are likely to undergo directional physical stress[21] due to macromolecular crowding, cytoplasmic streaming,[22] and cellular compartmentalization. Proteins might be deformed by physical stress, and such deformation would reduce solubility and trigger protein aggregation. Protein aggregation in neurons is thought to be closely related to neurodegenerative diseases such as Alzheimer's and Parkinson's diseases. High-sensitivity Rheo-NMR can reveal the detailed rheological response of aggregation-prone proteins, which will contribute to elucidation of the mechanism by which pathological aggregates and fibrils form, thereby providing a better molecular understanding of the onset of these diseases.

ASSOCIATED CONTENT

Supporting Information

The Supporting Information is available free of charge on the ACS Publications website at DOI: 10.1021/acs.analchem.7b01816.

Details of experimental methods including construction of the established Rheo-NMR instrument, NMR measurements and analysis, shear-induced peak volume decrease and chemical shift changes, mapping of the residues where chemical shift differences were observed between static and sheared conditions, and a table showing the rotational diffusion tensor parameters (PDF)

AUTHOR INFORMATION

Corresponding Author

*E-mail: sugase@moleng.kyoto-u.ac.jp.

ORCID

Daichi Morimoto: 0000-0002-7672-2136
Erik Walinda: 0000-0003-1882-6401
Kenji Sugase: 0000-0001-8623-7743

Author Contributions

The manuscript was written through contributions of all authors.

Notes

The authors declare no competing financial interest.

ACKNOWLEDGMENTS

We thank Seki Lee for the electron microscopy experiments. This work was supported by the John Mung Program for Young Scholars, the Uehara Memorial Foundation, the Shimadzu Science Foundation, the Mizuho Foundation for the Promotion of Sciences, JSPS KAKENHI (Grant Numbers JP16K18503 and JP26119004), and Interdisciplinary Research Promotion Project of the National Institutes of Natural Sciences (NINS) (Grant Number R281002).

DOI: 10.1021/acs.analchem.7b01816
Anal. Chem. 2017, 89, 7286–7290

REFERENCES

(1) Hill, E. K.; Krebs, B.; Goodall, D. G.; Howlett, G. J.; Dunstan, D. E. *Biomacromolecules* **2006**, *7* (1), 10−13.
(2) Dunstan, D. E.; Hamilton-Brown, P.; Asimakis, P.; Ducker, W.; Bertolini, J. *Soft Matter* **2009**, *5* (24), 5020−5028.
(3) Bekard, I. B.; Dunstan, D. E. *J. Phys. Chem. B* **2009**, *113* (25), 8453−8457.
(4) Nakatani, A. I.; Poliks, M. D.; Samulski, E. T. *Macromolecules* **1990**, *23* (10), 2686−2692.
(5) Schmidt, C. *Modern Magnetic Resonance*; Springer, 2006; pp 1515−1521.
(6) Medronho, B.; Schmidt, C.; Olsson, U.; Miguel, M. G. *Langmuir* **2010**, *26* (3), 1477−1481.
(7) Medronho, B.; Rodrigues, M.; Miguel, M. G.; Olsson, U.; Schmidt, C. *Langmuir* **2010**, *26* (13), 11304−11313.
(8) Medronho, B.; Olsson, U.; Schmidt, C.; Galvosas, P. *Z. Phys. Chem.* **2012**, *226* (11−12), 1293−1313.
(9) Böhme, U.; Scheler, U. *ACS Symp. Ser.* **2011**, *1077*, 431−438.
(10) Ohgo, K.; Bagusat, F.; Asakura, T.; Scheler, U. *J. Am. Chem. Soc.* **2008**, *130* (12), 4182−4186.
(11) Edwards, P. J.; Kakubayashi, M.; Dykstra, R.; Pascal, S. M.; Williams, M. A. *Biophys. J.* **2010**, *98* (9), 1986−1994.
(12) Britton, M. M.; Callaghan, P. T.; Kilfoil, M. L.; Mair, R. W.; Owens, K. M. *Appl. Magn. Reson.* **1998**, *15* (3−4), 287−301.
(13) Brox, T. I.; Douglass, B.; Galvosas, P.; Brown, J. R. *J. Rheol.* **2016**, *60* (5), 973−982.
(14) Berlin, K.; Longhini, A.; Dayie, T. K.; Fushman, D. *J. Biomol. NMR* **2013**, *57* (4), 333−352.
(15) Morimoto, D.; Walinda, E.; Fukada, H.; Sou, Y. S.; Kageyama, S.; Hoshino, M.; Fujii, T.; Tsuchiya, H.; Saeki, Y.; Arita, K.; Ariyoshi, M.; Tochio, H.; Iwai, K.; Namba, K.; Komatsu, M.; Tanaka, K.; Shirakawa, M. *Nat. Commun.* **2015**, *6*, 6116.
(16) Knowles, T. P.; Waudby, C. A.; Devlin, G. L.; Cohen, S. I.; Aguzzi, A.; Vendruscolo, M.; Terentjev, E. M.; Welland, M. E.; Dobson, C. M. *Science* **2009**, *326* (5959), 1533−1537.
(17) Chiti, F.; Dobson, C. M. *Nat. Chem. Biol.* **2009**, *5* (1), 15−22.
(18) Jahn, T. R.; Parker, M. J.; Homans, S. W.; Radford, S. E. *Nat. Struct. Mol. Biol.* **2006**, *13* (3), 195−201.
(19) Singh, I.; Themistou, E.; Porcar, L.; Neelamegham, S. *Biophys. J.* **2009**, *96* (6), 2313−2320.
(20) Deng, W.; Xu, Y.; Chen, W.; Paul, D. S.; Syed, A. K.; Dragovich, M. A.; Liang, X.; Zakas, P.; Berndt, M. C.; Di Paola, J.; Ware, J.; Lanza, F.; Doering, C. B.; Bergmeier, W.; Zhang, X. F.; Li, R. *Nat. Commun.* **2016**, *7*, 12863.
(21) Iwasaki, T.; Wang, Y. L. *Biophys. J.* **2008**, *94* (5), L35−L37.
(22) Niwayama, R.; Shinohara, K.; Kimura, A. *Proc. Natl. Acad. Sci. U. S. A.* **2011**, *108* (29), 11900−11905.

DOI: 10.1021/acs.analchem.7b01816
Anal. Chem. 2017, 89, 7286−7290